THE JOURNAL OF PHYSICAL CHEMISTRY C

Article

pubs.acs.org/JPCC

Spatial Structure of Electrical Diffuse Layers in Highly Concentrated Electrolytes: A Modified Poisson−Nernst−Planck Approach

Arik Yochelis*

Department of Solar Energy and Environmental Physics and Ben-Gurion National Solar Energy Center, Swiss Institute for Dryland Environmental and Energy Research, Jacob Blaustein Institutes for Desert Research (BIDR), Ben-Gurion University of the Negev, Sede Boqer Campus, Midreshet Ben-Gurion 84990, Israel

ABSTRACT: Studies of room-temperature ionic liquids showed that electrical diffuse layers in these highly concentrated electrolytes may exhibit spatially extended nonmonotonic (oscillatory) and monotonic decays. These unconventional properties are fundamentally different from traditional (dilute) electrolytes and demonstrate the limited mechanistic understanding of highly concentrated electrolytes. Moreover, electrolyte behavior placed in close proximity of two charged surfaces becomes even more unclear due to the possible overlap between diffuse layers. The latter is important as many applications require confinement into narrow spaces, e.g., energy and lubrication related applications. To advance the understanding of electrical diffuse layers in highly concentrated electrolytes (and ionic liquids) we use a semiphenomenological modified Poisson−Nernst−Planck equation and regulate weak dilutions. Using spatial dynamics methods and numerical computations, we analyze distinct diffuse layer characteristics (nonmonotonic and monotonic) and provide for each type the analytic conditions and the validity limits in terms of applied voltage, domain size, molecular packing, and short-range electrostatic correlations. We also discuss the qualitative generality of the results and thus believe that these insights will allow us to advance the electrochemical understanding of confined highly concentrated electrolytes and their technological applications.

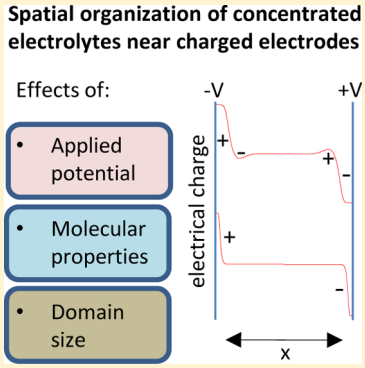

INTRODUCTION

The efficiency of electrochemical renewable energy devices, e.g., solar cells, supercapacitors, batteries, and fuel cells, is largely determined by electrolyte and solid/liquid interface properties. The former facilitate charge transport, while the latter are responsible for charge transfer or capacitance (charge/discharge cycling). In general, electrolyte properties near solid charged interfaces rely on a standard electrochemical theory developed for dilute electrolytes[1,2] in which ions are regarded as isolated point charges in a fluid carrier. In this view, under electrical field, ions of opposite charge are attracted toward the respectively charged electrodes and in the absence of chemical or charge transfer reactions screen the induced electrical field by forming an electrical diffuse layer (EDL).[3,4] The spatial extent of the emergent EDL is characterized by density of these charges (Poisson−Boltzmann theory), which is being reduced toward the bulk with a characteristic Debye length scale of typically nanometer size. As such, electrode screening by the electrolyte indicates the balance between the charge migration that is induced due to imposed surface charging and diffusion. Consequently, understanding of the EDL properties is important to charge transfer processes.[5,6]

Improvement of electrochemical applications often requires high charge density and increased active surface area.[7] The latter implies that the electrolyte will be confined in narrow spaces, specifically when interfaced with nanostructured electrodes, e.g., in supercapacitors and dye-sensitized solar cells. Hereby, both charge density and geometrical confinements fundamentally change the physicochemical intuition developed for traditional (dilute) electrolytes, as was demonstrated by room-temperature ionic liquids (RTILs):[8−15] (i) finite size effects of ions and electrostatic correlations are dominant[16−21] and (ii) small separation distances inheritably facilitate overlap between EDLs and thus are also sensitive to electrode structure.[22−25] RTILs (also referred to as solvent-free electrolytes or molten salts) become attractive for electrochemical applications not only due to their high charge density but also for their tunable anion/cation design, negligible vapor pressure, and wide electrochemical windows.[7,13,14,26−29] In general, these advantages make RTILs also attractive for other types of applications,[8−14,27,30−34] such as lubrication, nanoparticle synthesis, field-effect transistors, and drug delivery.

A fundamental and yet unclear characteristic of RTILs concerns unconventional spatial organizations of anions and cations near the liquid/solid interfaces,[8−15] i.e., the spatial structure of EDLs. Several recent studies have shown that the EDL structure in RTILs is profoundly different from that in traditional electrolytes, examples of which include camel shapes of the differential capacitance vs voltage curves[35−41] and self-assembled charge layering.[24,28,42−52] Charge layering near the liquid/solid interface can be viewed as a spatially oscillatory (nonmonotonic) EDL, displaying an alternating segregation of cations and anions that decay toward the bulk region. For metal

Received: December 25, 2013
Revised: February 16, 2014
Published: March 11, 2014

surfaces, this layering has been attributed to "overscreening" of the electrode potential.[19,21,53] On the other hand, it was recently shown that RTILs may also bare similarity to dilute electrolytes,[54,55] where a decrease in conductivity and monotonic decay of the EDL was attributed to ion association/dissociation kinetics.

Consequently, it appears that there are considerable knowledge gaps in the mechanistic understanding of highly concentrated electrolytes (and specifically RTILs) partly due to limited theoretical development that hinder rational interpretations of empirical results.[56,57] Ideally, the physicochemical complexity should capture several energy scales and short-/long-range interactions, e.g., electrostatic, van der Waals, hydrogen bonds.[58] However, as in many other complex systems (e.g., biological or environmental media), a detailed or ab initio theory that allows intuitive theoretical progress as well as spatiotemporal computational simplicity is not available. A plausible compromise was attempted by Bazant et al.[19,20] who proposed modifications to the widely exploited electrochemical Poisson−Nernst−Planck (PNP) equations by inclusion of steric effects[59−62] and electrostatic correlations.[16,21,63] Although the model is indeed semiphenomenological and simplified in the sense that it is based on local density approximations, it captured correctly trends obtained by more detailed computations,[20] including the rationale of empirically observed double-layer differential capacitance[19,64] and even motivating insights into RTIL/dielectric liquid interfaces.[34] Furthermore, mathematical and computational simplicity make the model feasible to electrochemical methods due to tractable temporal analysis.[65,66]

In a previous paper,[66] we showed via a modified PNP model[19,20,65] why confined RTILs can exhibit either oscillatory (spatial layering) or monotonic EDL structure. Here we provide details and show analytically how the spatial EDL structure depends on applied voltage, electrostatic correlations, molecular packing, and separation between inert electrodes. We employ a top-to-bottom approach in the sense that we start with the highly concentrated case (fully dissociated RTILs) and discuss the effect of dilation. In reality, RTILs can be diluted by organic solvents, such as propylene carbonate, ethylene carbonate, dimethyl carbonate, diethyl carbonate, and ethylmethyl carbonate[67−69] or by the control of ion dissociation.[54] The analysis combines numerical integrations and analytical methods of spatial dynamics. The latter allows identifications of conditions that lead to global attractors, heteroclinic cycles, that imply universal properties of highly concentrated electrolytes. The results thus provide a guiding tool to control the EDL structure for highly concentrated electrolytes under confinement. The paper is organized as following: At first we provide a brief overview of the modified PNP equations, and then we analyze the contributions of the bulk and the condensed charge layer near the electrodes, to the EDL structure. Finally we conclude and provide guiding relations for empirical control of EDLs.

FROM DILUTE TO CONCENTRATED ELECTROLYTES

Partial differential equations describing the charge transport/transfer are powerful complementary tools to electrochemical measurements since they employ a relatively simple framework (as compared to computationally exhaustive molecular dynamics and density functional theory methods) that allows analytical investigations and consequently basic intuitive rationale.[1,3,19,65] Next, we describe the model equations that will be used here to study the EDL emergence in highly concentrated electrolytes.

Modified Poisson−Nernst−Planck Framework. A binary 1:1, dilute electrolyte can be described by a mean-field approximation, in which ions are regarded as point charges and the electrical field is self-consistently determined by the charge density in the medium. The ionic transport (with identical anion/cation mobilities) is described by the continuity equation, which is also known as the Nernst−Planck formulation, while the electrostatics is given by the Poisson equation, together comprising the PNP equations[1,3]

$$\frac{\partial C_{\pm}}{\partial t} = -\nabla\cdot\mathbf{J}^{C_{\pm}} = D_{\pm}\nabla\cdot\left(\nabla C_{\pm} \pm \frac{F}{RT}C_{\pm}\nabla\phi\right) \tag{1a}$$

$$\nabla\cdot(\varepsilon\nabla\phi) = -F(C_{+} - C_{-}) \tag{1b}$$

In eq 1, $C_{\pm}$ are the positive and the negative charge densities, respectively; ϕ is the electrostatic potential; $D_{+} = D_{-} = D$ are the diffusion coefficients; R is the ideal gas constant; T is the absolute temperature; F is the Faraday constant; and ε is the dielectric permittivity of the medium.

The electrolyte (with constant dielectric permittivity) placed in between two charged planar and inert electrodes (separated by L) can be approximated by a one space dimensional variant of eq 1, i.e., $C_{\pm}(x,t)$ and $\phi(x)$, with respective boundary conditions (BCs) at $x = \pm\tilde{L}/2$, given by

$$J^{C_{\pm}} = 0 \tag{2a}$$

$$\phi = \pm\tilde{V} \tag{2b}$$

Initially at $t = 0$ the ions are equally distributed in space so that the whole domain is electroneutral, $C_{\pm}(x, 0) = C_0$. Once an external potential is applied ($t > 0$), ions move retrogradely toward oppositely charged electrodes and form a diffuse layer to screen the induced electrical field, so that far from each electrode electroneutrality is preserved. Specifically, the ion density and the potential within the diffuse layer decay monotonically (exponentially) toward the bulk with a characteristic Debye (screening) length, $\lambda_D = \varepsilon RT/(2F^2C_0)^{1/2}$. Consequently, in dilute electrolytes the Debye length is used as a measure of the spatial extent of the EDL.[1]

For highly concentrated electrolytes (where ions are no longer viewed as point charges), such as RTILs, appropriate modifications are required.[3] Many empirical observations have shown that EDLs in RTILs differ from those described by the classical PNP theory (eq 1), and therefore they are subjected to a variety of modeling and computational investigations[18−21,24,41,62,65,70−72] including molecular dynamics (MD), Monte Carlo (MC), and density functional theory (DFT). Motivated by unconventional capacitance observations, RTIL modeling incorporated, at first, finite size effects (i.e., steric interactions) into the PNP framework.[41,53,72] Steric interactions[59−62] are known to lead to a broadening of the compact layer near the electrodes (composed of only cations or anions), a so-called "crowding" effect. In this context, the ionic fluxes in eq 1 are modified by[19,60]

$$J^{\pm} = J_x^{C_{\pm}} - D\frac{\gamma C_{\pm}}{1 - \gamma(C_{+} + C_{-})}\frac{\partial}{\partial x}(C_{+} + C_{-}) \tag{3a}$$

where γ is the minimum volume available in space for ions (molecular packing). Steric effects, however, do not capture the

dx.doi.org/10.1021/jp412616f | J. Phys. Chem. C 2014, 118, 5716−5724

overscreening effects (spatial charge layering) that were observed in RTILs.[24,28,42−52] Here Bazant et al.[19] have proposed an additional semiphenomenological modification: electrostatic potential was modified to describe dielectric response associated with correlated ion pairs (short-range electrostatic correlations)[16,17,21,63]

$$\varepsilon\left(l_e^2\frac{\partial^2}{\partial x^2}-1\right)\frac{\partial^2\phi}{\partial x^2}=F(C_+-C_-) \tag{3b}$$

where l_e is the electrostatic correlation length. The left-hand side of the equation is interpreted as a dielectric response in the charge rearrangement,[20] with an effective permittivity operator defined by the displacement field, $\mathbf{D}=-\hat{\varepsilon}\partial_x\phi$, $\partial_x\mathbf{D}=F(C_+-C_-)$, and $\hat{\varepsilon}=\varepsilon(1-l_e^2\partial_{xx})$. The permittivity operator is suggested to describe a nonlinear response in symmetry breaking systems, i.e., due to confinement. For further details and model verifications we refer the reader to Story and Bazant.[20]

2. Nondimensionalization and Control Parameters. Before turning to analysis, we perform nondimensionalization by introducing the following scales and dimensionless variables: $\hat{x}=x/\lambda_D$, $\hat{t}=t/\tau$, $c=(C_++C_-)/(2C_0)$, $\rho=(C_+-C_-)/(2C_0)$, $\varphi=\phi/\phi_0$, where $\tau=\lambda_D^2/D$ and $\phi_0=RT/F$. Substituting into eq 1 and 3 and dropping the hats, the dimensionless modified PNP model reads

$$\frac{\partial c}{\partial t}=-\frac{\partial}{\partial x}J^C=\frac{\partial}{\partial x}\left(\frac{\partial c}{\partial x}+\rho\frac{\partial\varphi}{\partial x}+\frac{\nu c}{1-\nu c}\frac{\partial c}{\partial x}\right) \tag{4a}$$

$$\frac{\partial \rho}{\partial t}=-\frac{\partial}{\partial x}J^\rho=\frac{\partial}{\partial x}\left(\frac{\partial \rho}{\partial x}+c\frac{\partial\varphi}{\partial x}+\frac{\nu \rho}{1-\nu c}\frac{\partial c}{\partial x}\right) \tag{4b}$$

$$\left(l_c^2\frac{\partial^2}{\partial x^2}-1\right)\frac{\partial^2\varphi}{\partial x^2}=\rho \tag{4c}$$

where $\nu=2\gamma C_0$ and $l_c=l_e/\lambda_D$. The supplementary BCs at $x=\pm L/2$ are given by[19,20,65]

$$J^C=J^\rho=0 \tag{5a}$$

$$\varphi=\pm V \tag{5b}$$

$$\frac{\partial^3\varphi}{\partial x^3}=0 \tag{5c}$$

where $L=\tilde{L}/\lambda_D$ and $V=\tilde{V}/\phi_0$.

Equation 4 describe two generalized features of highly concentrated electrolyte properties:[19] $\nu\le 1$ stands for the ratio of the bulk ion density to the maximum possible density and l_c that can be effectively thought of as a dilution measure. The latter becomes significant for dilution of RTILs following experiments which suggested that molten salts behave like dilute electrolytes.[54,55] For fully dissociated ions of RTILs $\lambda_D\sim$ Å $<l_e\sim$ nm leading to $l_c>1$. However, if RTILs are indeed only partially dissociated,[54,55] λ_D increases toward the nanometer size, and since electrostatic correlations bounded by the Bjerrum length are also about nanometer size (due to large ion sizes), l_c significantly decreases and marks the weak electrolyte limit,[17] i.e., $l_c\le 1$. In the next section we will use l_c, V, and L as control parameters and show how characteristic relationships between these parameters shape the EDL structure.

ELECTRICAL DIFFUSE LAYER STRUCTURE

In reality, technological (e.g., electrochemical) devices impose distinct spatial scales for which the EDL structure becomes crucial,[22] such as overlap between EDLs in small separating distances. Besides the external constraints such as applied voltage and confinement, the EDL structure in RTILs is also subjected to contributions from molecular interactions designated here by l_c and ν. Under weak applied voltages ($\Delta V\le 1$) and large separation distances ($L\gg 1$), the emerged EDLs exhibit spatial oscillations (charge layering) as long as $l_c>0.5$ and monotonic decay otherwise.[20] This happens since the ionic bulk density exhibits only minor deviations from the initial equilibrium conditions so that bulk electroneutrality would prevail.[66]

Once applied voltage is increased [$\Delta V\sim O(10)$] and/or the separation distance is decreased [$L\sim O(100)$], one observes a relation[66] between the ion/charge saturation (due to steric effects) and the overscreening (due to electrostatic correlations): attraction and accumulation of charges at the electrodes and the respective depletion in the bulk. These are demonstrated by numerical integrations of eqs 4 and 5 in Figure 1. The initial conditions in all numerical integrations are $(c,\rho,\phi)=(1,0,0)$. Numerical solutions admit a front-like structure between the plateau in ionic and charge densities near the boundaries (electrodes) and the bulk region. The resulting plateau is due to steric (finite size) effects that admit an upper limit to ionic density and depend on molecular properties through ν (as will be shown next). It is also evident that the width of the plateau near the interface increases with the applied voltage.[19] For the sake of the analysis, we further simplify the system by assuming a sharp interface limit in which each plateau near the boundary has a width of χ and investigate the respective EDL structure for two cases:

(i) moderate thickness EDL for which $2\chi/(L-2\chi)\ll 1$;

(ii) thick EDL for which $2\chi/(L-2\chi)\sim O(1)$.

Case (i): Spatially Moderate Thickness EDLs. To study the characteristics of the moderate thickness EDL structure, namely, under which conditions EDL develops either nonmonotonic (spatial oscillations) or monotonic decay, we employ spatial dynamics methods. The focus is on the bulk and the saturated plateaus near the electrodes (i.e., boundaries). In the standard theory of dilute electrolytes bulk is not analyzed since it has passive properties. However, as we will show, highly concentrated electrolytes show differently—bulk has a hidden structure that is stabilized once external voltage (ΔV) is applied. The situation is similar to reaction−diffusion−migration systems for which spatial bulk properties strongly depend on BCs in a fashion that the latter select one of the possible states of the system.[73,74] Thus, the knowledge about the spatial bulk properties provides important information about asymptotic solutions to the whole system. Similar methods have been also applied to electrochemical systems under charge regulation.[23]

Spatial Dynamics and Asymptotic Behavior. Since fluxes J^C and J^ρ are conserved, it is convenient to rewrite eq 4 together with $E=-\partial_x\varphi$, as a set of ordinary differential equations

$$\frac{d\mathbf{v}}{dx}=\mathbf{T}^{-1}\mathbf{M}\mathbf{v}=\mathbf{N}\mathbf{v} \tag{6}$$

where

dx.doi.org/10.1021/jp412616f | J. Phys. Chem. C 2014, 118, 5716−5724

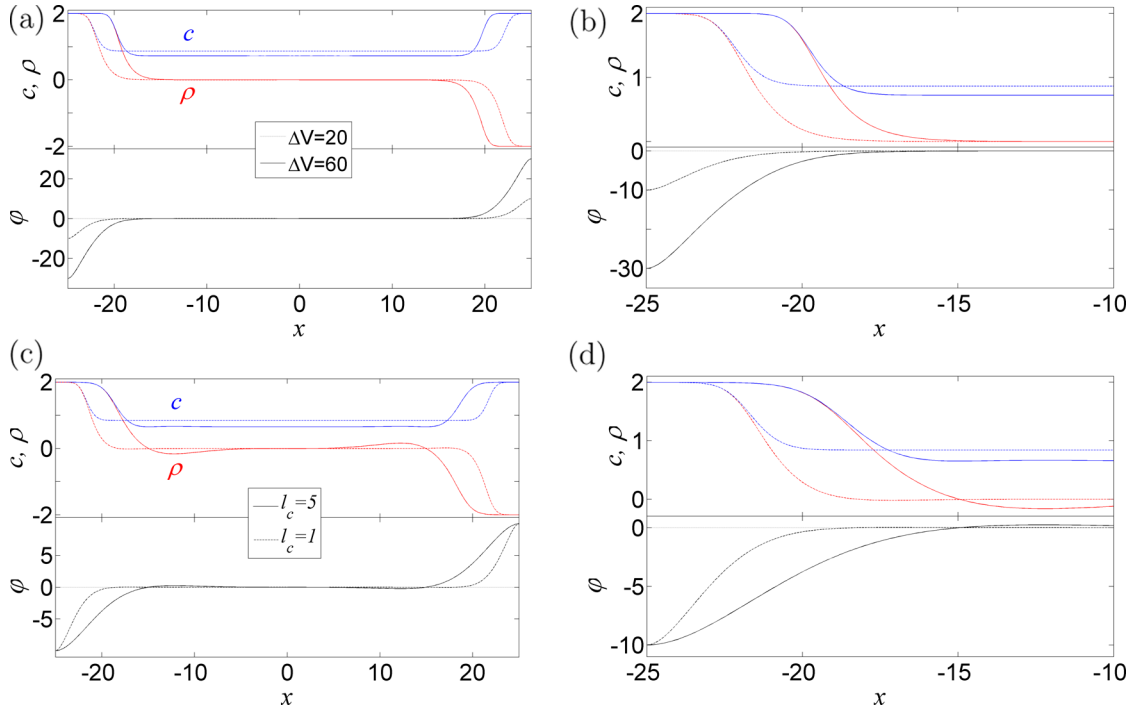

Figure 1. (a) and (c) demonstrate characteristic asymptotic profiles of (c,ρ,φ) obtained via eqs 4 and 5. (b) and (d) show a zoom in into the EDL region, and the dotted line is a guide to the eye for $\varphi = 0$. Equations 4 and 5 were integrated numerically with $\nu = 0.5$, $L = 50$, (a,b) $l_c = 0.6$, (c,d) $V = 10$, and other parameters as indicated in the figures (a) and (c), respectively.

$$\mathbf{T} = \begin{pmatrix} 1 & 0 & 0 & 0 & 0 \\ \frac{\nu\rho}{1-\nu c} & 1 & 0 & 0 & 0 \\ 0 & 0 & 1 & 0 & 0 \\ 0 & 0 & 0 & 1 & 0 \\ 0 & 0 & 0 & 0 & 0 \end{pmatrix}$$

$$\mathbf{M} = \begin{pmatrix} 0 & (1-\nu c)E & 0 & 0 & 0 \\ E & 0 & 0 & 0 & 0 \\ 0 & 0 & 0 & 1 & 0 \\ 0 & 0 & 0 & 0 & 1 \\ 0 & -l_c^{-2} & 0 & -l_c^{-2} & 0 \end{pmatrix}$$

$$\mathbf{N} = \begin{pmatrix} 0 & (1-\nu c)E & 0 & 0 & 0 \\ E & -\nu\rho E & 0 & 0 & 0 \\ 0 & 0 & 0 & 1 & 0 \\ 0 & 0 & 0 & 0 & 1 \\ 0 & -l_c^{-2} & 0 & -l_c^{-2} & 0 \end{pmatrix}$$

$$\mathbf{v} = \begin{pmatrix} c \\ \rho \\ E \\ u \\ w \end{pmatrix}$$

As will be shown next, eq 6 allows an efficient investigation of the asymptotic EDL structure. First, we analyze the spatial properties of the bulk and next show how BCs and domain size affect (together with the bulk) the EDL nature. Notably, empirical accessibility makes applied voltages and domain size as preferable control parameters and thus will be employed in what follows.

Bulk Region. In the absence of applied potential, i.e., assuming an infinite bulk, eq 6 admits a continued set of uniform states $\mathbf{v}_0 = (c, \rho, E, u, w)^T = (c^*, 0, 0, 0, 0)^T$, where the superscript stands for transpose. Ionic density c^* is allowed to vary due to depletion of ions once the voltage is applied, as shown in Figure 1. Weak spatial deviations about the uniform bulk state can be viewed in this framework as a spatial "instability".[73,75] Here space takes the form of a time-like variable, and the midplane ($x = 0$) is thought of as an initial condition with respect to dynamical systems (i.e., $t = 0$). Such an analogue allows us to determine the spatial deviation nature from $x = 0$ toward $x \to \pm\infty$ and eventually characterization of the EDL decay toward the bulk, a.k.a., spatial dynamics.

We perform a linear analysis by expanding first the solution to eq 6 as

$$\mathbf{v} = \mathbf{v}_0 + \delta\mathbf{v}_1 e^{\lambda x} + \delta^2\mathbf{v}_2 + \cdots \tag{7}$$

where $|\delta| \ll 1$ is an auxiliary parameter. By substituting eq 7 into eq 6, one obtains at the leading order in δ

$$\lambda\mathbf{v}_1 = \mathbf{J}_\mathbf{N}(c, \rho, E, u, w)\mathbf{v}_1 \tag{8}$$

where $\mathbf{J}_\mathbf{N}(c, \rho, E, u, w)$ is the Jacobian matrix of $\mathbf{N}$. Taking the determinant

$$|\mathbf{J}_\mathbf{N}(c, \rho, E, u, w) - \lambda\mathbf{I}| = 0 \tag{9}$$

and solving for λ, we obtain five eigenvalues

$$\lambda_0 = 0 \tag{10a}$$

$$\lambda_\pm^2 = \frac{1}{2l_c^2}(1 \pm \sqrt{1 - 4l_c^2 c^*}) \tag{10b}$$

dx.doi.org/10.1021/jp412616f | J. Phys. Chem. C 2014, 118, 5716−5724

As expected, λ_0 corresponds to the translational invariance of the ionic bulk concentration (c^*). The other four eigenvalues are either real or complex conjugated according to

$$l_c^* = \frac{1}{2\sqrt{c^*}} \tag{11}$$

We note that eigenvalues $\lambda_\pm$ are identical to an ansats that was used by Storey and Bazant[20] for the limiting case of weak electrolytes ($\Delta V < 1$ and $c^* = 1$).

Criterion 11, along with the distinct configurations of the spatial eigenvalues, is presented in Figure 2. At $l_c = l_c^*$ (middle inset), the eigenvalues take the double multiplicity at both sides of the real axis, i.e., $\lambda_+ = -\lambda_-$. For $l_c < l_c^*$ (left inset), all eigenvalues are real, while for $l_c > l_c^*$ (right inset), the eigenvalues are complex conjugated. In practice, applied voltages induce antisymmetric $[\varphi(x) = -\varphi(-x)]$ force with respect to $x = 0$ which is responsible for the ion depletion in the bulk, i.e., change in c^*. In this respect Im $\lambda_\pm$ are viewed as wavenumbers where the real eigenvalues correspond to a monotonic approach toward $x \to 0^\pm$, and complex conjugated eigenvalues correspond to spatially decaying oscillations (charge layering). Consequently, estimation of c^* becomes paramount since it determines the form of the spatial decay and will be discussed next.

Plateau Region near the Solid/Liquid Interface. Due to charge conservation, the depletion level of the ion density in the bulk depends mainly on the width of the plateau region near the boundaries, while the plateau width depends on the applied voltage, as demonstrated in Figure 1. Notably, while c and ρ exhibit saturation and thus form an interface (front) between the plateau near the boundary and the bulk, the potential (ϕ) exhibits a distinct (larger) decay scale which is determined by ΔV. Using this scale separation, evaluation of the saturation plateau width (χ) will allow us eventually to determine the bulk ion density c^* and thus the EDL decay nature.

To estimate the plateau width, we rescale the space $\xi = x/L$ and rewrite eq 6 as

$$\frac{dc}{d\xi} = L(1 - \nu c)\rho E \tag{12a}$$

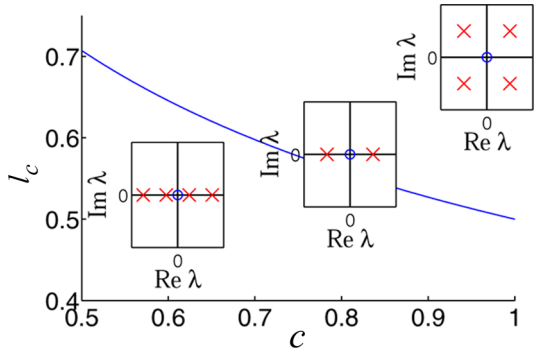

Figure 2. Parameter space showing the transition criterion 11 from nonmonotonic to monotonic spatial decay of EDL toward the bulk region. At the onset, the spatial eigenvalues correspond to one trivial (○) and a double multiplicity (×) at the real axis (middle inset). Above the onset, the real eigenvalues become complex (right inset) implying spatial oscillations, while below the onset the eigenvalues split and remain on the real axis (left inset) implying spatially monotonic decay. The eigenvalues are given by eq 10.

$$\frac{d\rho}{d\xi} = L(c - \nu\rho^2)E \tag{12b}$$

$$\frac{dE}{d\xi} = Lu \tag{12c}$$

$$\frac{du}{d\xi} = Lw \tag{12d}$$

$$\frac{l_c^2}{L}\frac{dw}{d\xi} = u - \rho \tag{12e}$$

Equation 12e admits distinct limits of the plateau thickness which correspond to the ratio between electrostatic correlations and the domain size, l_c^2/L.

For moderate plateau thickness $l_c^2/L \ll 1$, the left-hand side of eq 12e vanishes and leads to $|u| \sim |\rho|$ (sign of u and ρ depends on the BCs, see eq 5b). Now, since E varies over the plateau region, eqs 12a and 12b provide the saturation limit for the uniform solutions of ions and charges, $1 - \nu c = c - \nu\rho^2 = 0$, leading to $c = |\rho| = \nu^{-1}$. The latter within the plateau region allows to linearly approximate the electrical field $E \propto \xi$ (see eq 12c). Integrating over the plateau domain and rescaling back to x, we obtain

$$E = \nu^{-1}\chi \tag{13}$$

On the other hand, the electrical field within the plateau domain can also be approximated as capacitance, $E = \Delta V/(2\chi)$, which together with eq 13 yields

$$\chi = \sqrt{\frac{\Delta V\nu}{2}} \tag{14}$$

and consequently

$$c^* = \frac{L\nu - 2\sqrt{\nu\Delta V/2}}{\nu(L - 2\sqrt{\nu\Delta V/2})} \tag{15}$$

The moderate plateau thickness limit provides via eq 15 an additional scale $\eta \ll 1$ and a relation between applied voltage and domain size, $\eta = (\Delta V/2)^{1/2}/L$

$$c^* \simeq 1 - 2\frac{1 - \nu}{\sqrt{\nu}}\eta - 4(1 - \nu)\eta^2 \tag{16}$$

In Figure 3, we show that eq 16 agrees well with direct numerical solutions of eq 4 (we avoid plotting eq 15 since the results (in this range) are quite indistinguishable). Notably, by combining eqs 15 and 11 we can also approximate the critical applied voltage that indicates the transition from monotonic to nonmonotonic EDL

$$\Delta V_c \sim \frac{\nu L^2}{2}\left(\frac{1 - 4l_c^2}{\nu - 4l_c^2}\right)^2 \tag{17}$$

The above derivations clarify the connection between the ionic reduction in bulk $c = c^*$ and plateau widening (near the electrodes). Specifically, this connection indicates how different molecular and external system properties influence the decay of charges toward the bulk to be either monotonic or nonmonotonic (oscillatory). From a spatial dynamics point of view, the solutions take the form of a heteroclinic cycle-like connection[75] by replacing $x \to \pm\infty$ with $x \to 0^\pm$ (time-like reversal). Figure 4 shows an approach to a heteroclinic connection at $c = |\rho| = \nu^{-1}$, once the applied voltage is

dx.doi.org/10.1021/jp412616f | J. Phys. Chem. C 2014, 118, 5716−5724

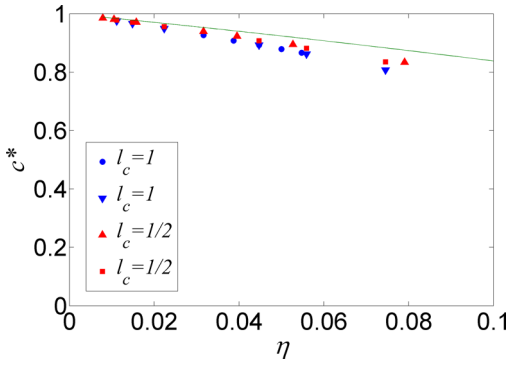

Figure 3. Comparison between the ionic bulk density obtained through numerical integration of eqs 4 and 5 (marked by symbols) and the approximated (solid line) form (eq 16) with $\nu = 0.5$. Several compositions of V and L were taken according to $\eta = (\Delta V/2)^{1/2}/L = V^{1/2}/L \ll 1$, i.e., $L \in [80,400]$ and $V \in [10,30]$, respectively.

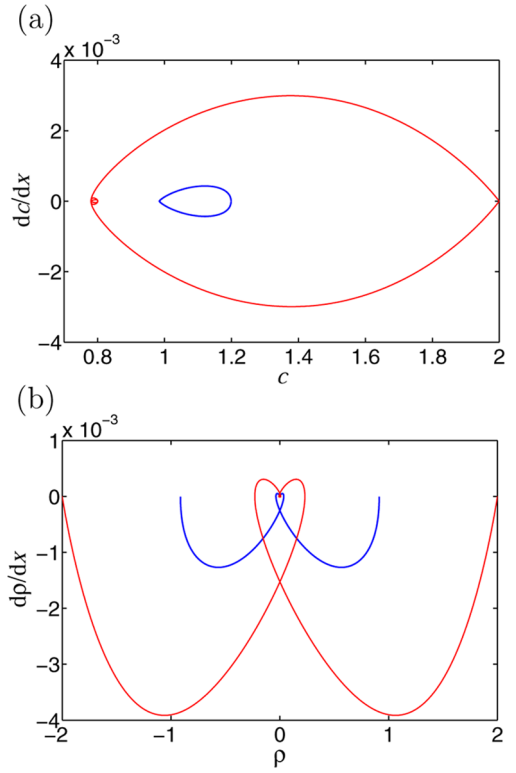

Figure 4. Phase plane representation for (a) ionic density and (b) charge density. Equations 4 and 5 were numerically integrated with $\nu = 0.5$, $l_c = 10$, and $L = 100$ with $V = 1$ (thick/dark line) and $V = 10$ (thin/light line).

increased; note that qualitatively similar behavior persists also for monotonic connections. Since heteroclinic cycles are global-phase plane flow attractors (here spatial flow is an analogue of temporal flow), they indeed imply that these unconventional connections between the boundary plateaus and the bulk regions, are general. This behavior has similarities to structural connections in multiphase systems[76] even though not all fields in solutions to eq 4 show approach to uniform states; i.e., the potential does not saturate near the boundaries, as shown in Figure 1. However, while potential depends on the spatial charge density, it in turn affects only the plateau widening via BC (see eq 5). Thus, even though not all fields approach uniform states, solutions to eq 4 can be viewed as heteroclinic connections.[75] Consequently, the described behavior is rather general and can be obtained by either changing electrostatic correlations (l_c), molecular packing (ν), applied voltage (ΔV), or domain size (L) as long as the moderate thickness limit is preserved, $l_c^2/L \sim (\Delta V/2)^{1/2}/L \ll 1$.

Case (ii): Spatially Thick EDLs. Once the applied voltage increases significantly and/or separation distance decreases, i.e., $l_c^2/L \sim (\Delta V/2)^{1/2}/L \sim O(1)$, the width of the plateau region becomes comparable with the extent of the bulk, $2\chi/(L - 2\chi) \sim 1$ and $c^* \to 1/2$, as shown in Figure 5. In this case, scale separation is invalid; however, the transition from oscillatory to monotonic behaviors still obeys eq 11. We demonstrate such a transition in Figure 5, where the separation distance is reduced from $L = 22$ to $L = 20$ for fixed $l_c = 1$ and $\Delta V = 20$. Notably, in such situations screening of the electrical field is impossible, and electroneutrality cannot be approached, as shown in the inset of Figure 5(b). Yet, charge and electrical field profiles can still be rationalized.

CONCLUSIONS

The growing interest in highly concentrated electrolytes and specifically RTILs stems from a broad range of potential technological applications, examples of which include electrochemical applications,[7,9,14,28] catalysis,[77−79] lubrication,[32,80−84] and nanoparticle stabilizations.[31,70,85−88] However, despite the wide empirical investigations, RTILs still impose fundamental challenges regarding the distinct spatial structures of EDLs and the respective conditions at which each type emerges: nonmonotonic (spatially oscillatory charge layering) decay[24,28,42−52] vs monotonic type.[54] To further discourse and advance the subject, we have chosen to study binary RTILs (solvent-free electrolytes) and regulated weak dilutions. For this purpose, we analyzed a modified PNP model suggested by

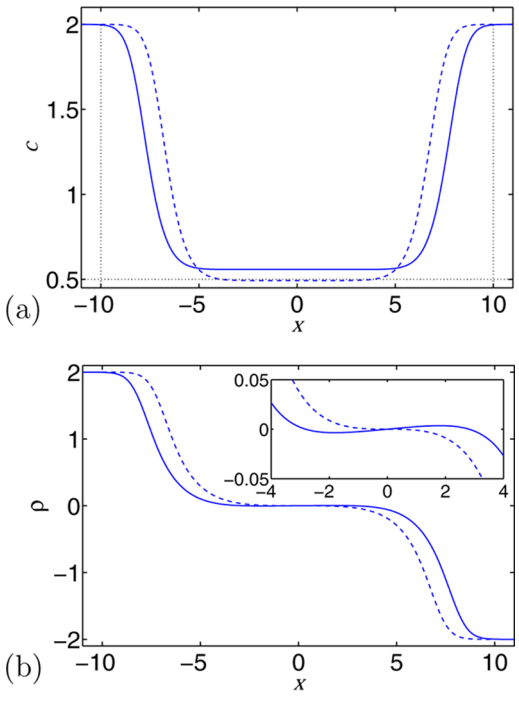

Figure 5. Ion density (a) and charge density (b) profiles, above (solid line) and below (dashed line) the onset. Equations 4 and 5 were numerically integrated with $V = 10$, $l_c = 1$, $\nu = 0.5$, $L = 22$ (solid line), and $L = 20$ (dashed line).

dx.doi.org/10.1021/jp412616f | J. Phys. Chem. C 2014, 118, 5716−5724

Bazant et al.[19] The advantage of this semiphenomenological simplified model is that it apparently captures the critical physicochemical basis for RTILs and is simple enough to allow analytic/numerical explorations.[20,65] Consequently, the model has the potential to produce a nonlinear intuition that extends the standard electrochemical theory of dilute electrolytes.[1−3]

Through asymptotic methods of spatial dynamics, we have analytically analyzed both moderate thickness EDLs (where the EDL width is much smaller than the bulk region) and thick EDLs (where the EDL widths are comparable with the bulk region); thin EDLs under weak potentials ($\Delta\tilde{V} < RT/F$) and large domains had been discussed elsewhere.[20,65] The analytical results were shown to agree well with direct numerical simulations of the full model system, eq 4. Specifically, we have shown that EDLs can exhibit either nonmonotonic or monotonic decays and identified the analytical conditions and validity limits in terms of applied voltage, domain size, molecular packing, and short-range electrostatic correlations. In addition, we showed the universal nature of the results, and as such we anticipate them to persist under inclusion of additional physicochemical modifications, such as ionic dissociation kinetics[54,55] or micellization.[53]

To summarize:

•The moderate thickness EDL can be expected providing $l_c^2/L \ll 1$ and $(\Delta V/2)^{1/2}/L \ll 1$ which, respectively, in real units read

$$\frac{\tilde{L}}{l_e^2\sqrt{C_0}} \gg \sqrt{\frac{2F^2}{\varepsilon RT}}, \quad \frac{\tilde{L}^2 C_0}{\Delta\tilde{V}} \gg \frac{1}{4}\frac{\varepsilon}{F}$$

•In the moderate EDL thickness limit, transition from nonmonotonic to monotonic decay of EDLs is anticipated after combining $l_c^2/L \ll 1$ and $l_c^* = 1/(2(c^*)^{1/2})$

$$\frac{\tilde{L}(C_+^{bulk} + C_-^{bulk})}{\sqrt{C_0}} \gg \frac{1}{2}\sqrt{\frac{\varepsilon RT}{2F^2}}$$

•In the thick EDL limit, transition from nonmonotonic to monotonic decay is anticipated about $l_c^* = 1/2^{1/2}$

$$l_e^*\sqrt{C_0} = \frac{\sqrt{\varepsilon RT}}{2F}$$

To this end, since EDL structure is very basic to technological applications,[8−14,27,30−32] we hope that the approach and results provided here will allow new vistas and guiding lines for further explorations of confined highly concentrated electrolytes.

AUTHOR INFORMATION

Corresponding Author

*E-mail: yochelis@bgu.ac.il.

Notes

The authors declare no competing financial interest.

ACKNOWLEDGMENTS

The author thanks Iris Visoly-Fisher (BIDR, Ben-Gurion University of the Negev) for helpful discussions.

REFERENCES

(1) Bard, A. J.; Faulkner, L. R. *Electrochemical Methods: Fundamentals and Applications*, 2nd ed.; John Willy & Sons, Inc.: USA, 2001.

(2) Macdonald, J. R. Impedance Spectroscopy - Old Problems and New Developments. *Electrochim. Acta* **1990**, *35*, 1483−1492.

(3) Bazant, M. Z.; Squires, T. M. Induced-charge Electrokinetic Phenomena. *Curr. Opin. Colloid Interface Sci.* **2010**, *15*, 203−213.

(4) Ben-Yaakov, D.; Andelman, D. Revisiting the Poisson-Boltzmann Theory: Charge Surfaces, Multivalent Ions and Inter-plate Forces. *Phys. A* **2010**, *389*, 2956−2961.

(5) Bazant, M. Z.; Thornton, K.; Ajdari, A. Diffuse-charge Dynamics in Electrochemical Systems. *Phys. Rev. E* **2004**, *70*, 021506.

(6) Dickinson, E. J.; Compton, R. G. Influence of the Diffuse Double Layer on Steady-state Voltammetry. *J. Electroanal. Chem.* **2011**, *661*, 198−212.

(7) MacFarlane, D. R.; Tachikawa, N.; Forsyth, M.; Pringle, J. M.; Howlett, P. C.; Elliott, G. D.; Davis, D. J. H.; Watanabe, M.; Simon, P.; Angell, C. A. Energy Applications of Ionic Liquids. *Energy Environ. Sci.* **2014**, *7*, 232−250.

(8) Silvester, D. S.; Compton, R. G. Electrochemistry in Room Temperature Ionic Liquids: A Review and Some Possible Applications. *Z. Chem. Phys.* **2006**, *220*, 1247−1274.

(9) Galinski, M.; Lewandowski, A.; Stepniak, I. Ionic Liquids as Electrolytes. *Electrochim. Acta* **2006**, *51*, 5567−5580.

(10) Nakagawa, H.; Fujino, Y.; Kozono, S.; Katayama, Y.; Nukuda, T.; Sakaebe, H.; Matsumoto, H.; Tatsumi, K. Application of Nonflammable Electrolyte with Room Temperature Ionic Liquids (rtils) for Lithium-ion Cells. *J. Power Sources* **2007**, *174*, 1021−1026.

(11) Zhu, Q.; Song, Y.; Zhu, X.; Wang, X. Ionic Liquid-based Electrolytes for Capacitor Applications. *J. Electroanal. Chem.* **2007**, *601*, 229−236.

(12) Simon, P.; Gogotsi, Y. Materials for Electrochemical Capacitors. *Nat. Mater.* **2008**, *7*, 845−854.

(13) Wishart, J. F. Energy Applications of Ionic Liquids. *Energy Environ. Sci.* **2009**, *2*, 956−961.

(14) Armand, M.; Endres, F.; MacFarlane, D. R.; Ohno, H.; Scrosati, B. Ionic-liquid Materials for the Electrochemical Challenges of the Future. *Nat. Mater.* **2009**, *8*, 621−629.

(15) Thorsmølle, V. K.; Rothenberger, G.; Topgaard, J. C.; Brauer, D.; Kuang, D.-B.; Zakeeruddin, S. M.; Lindman, B.; Graetzel, M.; Moser, J.-E. Extraordinarily Efficient Conduction in a Redox-active Ionic Liquid. *Chem. Phys. Chem.* **2011**, *12*, 145−149.

(16) Levin, Y. Electrostatic Correlations: From Plasma to Biology. *Rep. Prog. Phys.* **2002**, *65*, 1577−1632.

(17) Santangelo, C. D. Computing Counterion Densities at Intermediate Coupling. *Phys. Rev. E* **2006**, *73*, 041512.

(18) Skiner, B.; Loth, M. S.; Shklovskii, B. I. Capacitance of the Double Layer Formed at the Metal/Ionic-Conductor Interface: How Large Can It Be? *Phys. Rev. Lett.* **2010**, *104*, 128302.

(19) Bazant, M. Z.; Storey, B. D.; Kornyshev, A. A. Double Layer in Ionic Liquids: Overscreening versus Crowding. *Phys. Rev. Lett.* **2011**, *106*, 046102.

(20) Storey, B. D.; Bazant, M. Z. Effects of Electrostatic Correlations on Electrokinetic Phenomena. *Phys. Rev. E* **2012**, *86*, 056303.

(21) Lynden-Bell, R. M.; Frolov, A. I.; Fedorov, M. V. Electrode Screening by Ionic Liquids. *Phys. Chem. Chem. Phys.* **2012**, *14*, 2693−2701.

(22) Biesheuvel, P. M.; Fu, Y. Q.; Bazant, M. Z. Diffuse Charge and Faradaic Reactions in Porous Electrodes. *Phys. Rev. E* **2011**, *83*, 061507.

(23) Beaume, C.; Plouraboue, F.; Bergeon, A.; Knobloch, E. Electrolyte Stability in a Nanochannel with Charge Regulation. *Langmuir* **2011**, *27*, 11187−11198.

(24) Merlet, C.; Rotenberg, B.; Madden, P. A.; Taberna, P.-L.; Simon, P.; Gogotsi, Y.; Salanne, M. On the Molecular Origin of Supercapacitance in Nanoporous Carbon Electrodes. *Nat. Mater.* **2012**, *11*, 306−310.

(25) Ben-Yaakov, D.; Andelman, D.; Diamant, H. Interaction Between Heterogeneously Charged Surfaces: Surface Patches and Charge Modulation. *Phys. Rev. E* **2013**, *87*, 022402.

(26) Bai, Y.; Cao, Y.; Zhang, J.; Wang, M.; Li, R.; Wang, P.; Zakeeruddin, S. M.; Graetzel, M. High-performance Dye-sensitized Solar Cells Based on Solvent-free Electrolytes Produced from Eutectic Melts. *Nat. Mater.* **2008**, *7*, 626−630.

(27) Niedermeyer, H.; Hallett, J. P.; Villar-Garcia, I. J.; Hunt, P. A.; Welton, T. Mixtures of Ionic Liquids. *Chem. Soc. Rev.* **2012**, *41*, 7780−7802.
(28) Ohno, H. *Electrochemical Aspects of Ionic Liquids*, 2nd ed.; John Wiley & Sons, Inc.: Hoboken, NJ, 2005.
(29) Hapiot, P.; Lagrost, C. Electrochemical Reactivity in Room-Temperature Ionic Liquids. *Chem. Rev.* **2008**, *108*, 2238−2264.
(30) Plechkova, N. V.; Seddon, K. R. Applications of Ionic Liquids in the Chemical Industry. *Chem. Soc. Rev.* **2008**, *37*, 123−150.
(31) Dupont, J.; Scholten, J. D. On the Structural and Surface Properties of Transition-metal Nanoparticles in Ionic Liquids. *Chem. Soc. Rev.* **2010**, *39*, 1780−1804.
(32) Zhou, F.; Liang, Y.; Liu, W. Ionic Liquid Lubricants: Designed Chemistry for Engineering Applications. *Chem. Soc. Rev.* **2009**, *38*, 2590−2599.
(33) Fujimotoa, T.; Awaga, K. Electric-double-layer Field-effect Transistors with Ionic Liquids. *Phys. Chem. Chem. Phys.* **2013**, *15*, 8983−9006.
(34) Lee, D. W.; Im, D. J.; Kang, I. S. Electric Double Layer at the Interface of Ionic Liquid-Dielectric Liquid under Electric Field. *Langmuir* **2013**, *29*, 1875−1884.
(35) Zhou, W.; Inoue, S.; Iwahashi, T.; Kanai, K.; Seki, K.; Miyamae, T.; Kim, D.; Katayama, Y.; Ouchi, Y. Double Layer Structure and Adsorption/desorption Hysteresis of Neat Ionic Liquid on Pt Electrode Surface - An in-situ IR-visible Sum-frequency Generation Spectroscopic Study. *Electrochem. Commun.* **2010**, *12*, 672−675.
(36) Lockett, V.; Sedev, R.; Ralston, J.; Horne, M.; Rodopoulos, T. Differential Capacitance of The Electrical Double Layer in Imidazolium-based Ionic Liquids: Influence of Potential, Cation Size, and Temperature. *J. Phys. Chem. C* **2008**, *112*, 7486−7495.
(37) Islam, M. M.; Alam, M. T.; Ohsaka, T. Electrical Double-Layer Structure in Ionic Liquids: A Corroboration of the Theoretical Model by Experimental Results. *J. Phys. Chem. C* **2008**, *112*, 16568−16574.
(38) Alam, M. T.; Islam, M. M.; Okajima, T.; Ohsaka, T. Measurements of Differential Capacitance at Mercury/room-temperature Ionic Liquids Interfaces. *J. Phys. Chem. C* **2007**, *111*, 18326−18333.
(39) Alam, M. T.; Islam, M. M.; Okajima, T.; Ohsaka, T. Measurements of Differential Capacitance in Room Temperature Ionic Liquid at Mercury, Glassy Carbon and Gold Electrode Interfaces. *Electrochem. Commun.* **2007**, *9*, 2370−2374.
(40) Alam, M. T.; Islam, M. M.; Okajima, T.; Ohsaka, T. Capacitance Measurements in a Series of Room-Temperature Ionic Liquids at Glassy Carbon and Gold Electrode Interfaces. *J. Phys. Chem. C* **2008**, *112*, 16600−16608.
(41) Lauw, Y.; Horne, M. D.; Rodopoulo, T.; Leermakers, F. A. M. Room-temperature Ionic Liquids: Excluded Volume and Ion Polarizability Effects in The Electrical Double-layer Structure and Capacitance. *Phys. Rev. Lett.* **2009**, *103*, 117801.
(42) Carmichael, A.; Hardacre, C.; Holbrey, J.; Nieuwenhuyzen, M.; Seddon, K. Molecular Layering and Local Order in Thin Films of 1-alkyl-3-methylimidazolium Ionic Liquids Using X-ray Reflectivity. *Mol. Phys.* **2001**, *99*, 795−800.
(43) Fukushima, T.; Kosaka, A.; Ishimura, Y.; Yamamoto, T.; Takigawa, T.; Ishii, N.; Aida, T. Molecular Ordering of Organic Molten Salts Triggered by Single-walled Carbon Nanotubes. *Science* **2003**, *300*, 2072−2074.
(44) Buzzeo, M.; Evans, R.; Compton, R. Non-haloaluminate Room-temperature Ionic Liquids in Electrochemistry - A Review. *Chem. Phys. Chem.* **2004**, *5*, 1106−1120.
(45) Wang, Y. T.; Voth, G. A. Unique Spatial Heterogeneity in Ionic Liquids. *J. Am. Chem. Soc.* **2005**, *127*, 12192−12193.
(46) Lopes, J.; Padua, A. Nanostructural Organization in Ionic Liquids. *J. Phys. Chem. B* **2006**, *110*, 3330−3335.
(47) Atkin, R.; Warr, G. G. Structure in Confined Room-temperature Ionic Liquids. *J. Phys. Chem. C* **2007**, *111*, 5162−5168.
(48) Mezger, M.; Schroder, H.; Reichert, H.; Schramm, S.; Okasinski, J. S.; Schoder, S.; Honkimaki, V.; Deutsch, M.; Ocko, B. M.; Ralston, J.; et al. Molecular Layering of Fluorinated Ionic Liquids at A Charged Sapphire (0001) Surface. *Science* **2008**, *322*, 424−428.
(49) Ueno, K.; Kasuya, M.; Watanabe, M.; Mizukami, M.; Kurihara, K. Resonance Shear Measurement of Nanoconfined Ionic Liquids. *Phys. Chem. Chem. Phys.* **2010**, *12*, 4066−4071.
(50) Perkin, S. Ionic Liquids in Confined Geometries. *Phys. Chem. Chem. Phys.* **2012**, *14*, 5052−5062.
(51) Zhou, H.; Rouha, M.; Feng, G.; Lee, S. S.; Docherty, H.; Fenter, P.; Cummings, P. T.; Fulvio, P. F.; Dai, S.; McDonough, J.; et al. Nanoscale Perturbations of Room Temperature Ionic Liquid Structure at Charged and Uncharged Interfaces. *ACS Nano* **2012**, *6*, 9818−9827.
(52) Smith, A. M.; Lovelock, K. R. J.; Gosvami, N. N.; Licence, P.; Dolan, A.; Welton, T.; Perkin, S. Monolayer to Bilayer Structural Transition in Confined Pyrrolidinium-Based Ionic Liquids. *J. Phys. Chem. Lett.* **2013**, *4*, 378−382.
(53) Kornyshev, A. A. Double-layer in Ionic Liquids: Paradigm Change? *J. Phys. Chem. B* **2007**, *111*, 5545−5557.
(54) Gebbie, M. A.; Valtiner, M.; Banquy, X.; Fox, E. T.; Henderson, W. A.; Israelachvili, J. N. Ionic Liquids Behave as Dilute Electrolyte Solutions. *Proc. Natl. Acad. Sci. U.S.A.* **2013**, *110*, 9674−9679.
(55) Richey, F. W.; Dyatkin, B.; Gogotsi, Y.; Elabd, Y. Ion Dynamics in Porous Carbon Electrodes in Supercapacitors Using in situ Infrared Spectroelectrochemistry. *J. Am. Chem. Soc.* **2013**, *135*, 12818−12826.
(56) Perkin, S.; Salanne, M.; Madden, P.; Lynden-Bell, R. Is a Stern and Diffuse Layer Model Appropriate to Ionic Liquids at Surfaces? *Proc. Natl. Acad. Sci. U.S.A.* **2013**, *110*, E4121.
(57) Gebbie, M. A.; Valtinerb, M.; Banquyc, X.; Hendersond, W. A.; Israelachvili, J. N. Experimental Observations Demonstrate that Ionic Liquids Form Both Bound (Stern) and Diffuse Electric Double Layers. *Proc. Natl. Acad. Sci. U.S.A.* **2013**, *110*, E4122.
(58) Israelachvili, J. *Intermolecular and Surface Forces*, 3rd ed.; Academic Press: London, 2011.
(59) Bikerman, J. J. Structure and Capacity of Electrical Double Layer. *Philos. Mag. Ser. 7* **1942**, *33*, 384−397.
(60) Borukhov, I.; Andelman, D.; Orland, H. Steric Effects in Electrolytes: A Modified Poisson-Boltzmann Equation. *Phys. Rev. Lett.* **1997**, *79*, 435−438.
(61) Kilic, M. S.; Bazant, M. Z.; Ajdari, A. Steric Effects in The Dynamics of Electrolytes at Large Applied Voltages. I. Double-layer Charging. *Phys. Rev. E* **2007**, *75*, 021502.
(62) Hatlo, M. M.; van Roij, R.; Lue, L. The Electric Double Layer at High Surface Potentials: The Influence of Excess Ion Polarizability. *EPL* **2012**, *97*, 28010.
(63) Kornyshev, A. A.; Schmickler, W.; Vorotyntsev, M. A. Nonlocal Electrostatic Approach to The Problem of a Double-layer at a Metal-electrolyte Interface. *Phys. Rev. B* **1982**, *25*, 5244−5256.
(64) Fedorov, M. V.; Georgi, N.; Kornyshev, A. A. Double Layer in Ionic Liquids: The Nature of the Camel Shape of Capacitance. *Electrochem. Commun.* **2010**, *12*, 296−299.
(65) Zhao, H. Diffuse-charge Dynamics of Ionic Liquids in Electrochemical Systems. *Phys. Rev. E* **2011**, *84*, 051504.
(66) Yochelis, A. Transition from Non-monotonic to Monotonic Electrical Diffuse Layers: Impact of Confinement in Ionic Liquids. *Phys. Chem. Chem. Phys.* **2014**, *16*, 2836−2841.
(67) McEwen, A. B.; McDevitt, S. F.; Koch, V. R. Nonaqueous Electrolytes for Electrochemical Capacitors: Imidazolium Cations and Inorganic Fluorides with Organic Carbonates. *J. Electrochem. Soc.* **1997**, *144*, L84−L86.
(68) Krause, A.; Balducci, A. High Voltage Electrochemical Double Layer Capacitor Containing Mixtures of Ionic Liquids and Organic Carbonate as Electrolytes. *Electrochem. Commun.* **2011**, *13*, 814−817.
(69) Ruiz, V.; Huynh, T.; Sivakkumar, S. R.; Pandolfo, A. G. Ionic Liquid−solvent Mixtures as Supercapacitor Electrolytes for Extreme Temperature Operation. *RSC Adv.* **2012**, *2*, 5591−5598.
(70) Ueno, K.; Sano, Y.; Inaba, A.; Kondoh, M.; Watanabe, M. Soft Glassy Colloidal Arrays in an Ionic Liquid: Colloidal Glass Transition, Ionic Transport, and Structural Color in Relation to Microstructure. *J. Phys. Chem. B* **2010**, *114*, 13095−13103.

(71) Gillespie, D.; Khair, A. S.; Bardhan, J. P.; Pennathur, S. Efficiently Accounting for Ion Correlations In Electrokinetic Nanofluidic Devices Using Density Functional Theory. *J. Colloid Interface Sci.* **2011**, *359*, 520−529.
(72) Oldham, K. B. A Gouy-Chapman-Stern Model of the Double Layer at a (metal)/(ionic Liquid) Interface. *J. Electroanal. Chem.* **2008**, *613*, 131−138.
(73) Yochelis, A.; Sheintuch, M. Principal Bifurcations and Symmetries in The Emergence of Reaction-Diffusion-Advection Patterns on Finite Domains. *Phys. Rev. E* **2009**, *80*, 056201.
(74) Yochelis, A.; Sheintuch, M. Towards Nonlinear Selection of Reaction-Diffusion Patterns in Presence of Advection: A Spatial Dynamics Approach. *Phys. Chem. Chem. Phys.* **2009**, *11*, 9210−9223.
(75) Knobloch, E. Spatially Localized Structures In Dissipative Systems: Open Problems. *Nonlinearity* **2008**, *21*, T45.
(76) Elphick, C.; Hagberg, A.; Meron, E. Multiphase Patterns in Periodically Forced Oscillatory Systems. *Phys. Rev. E* **1999**, *59*, 5285−5291.
(77) Welton, T. Room-temperature Ionic Liquids. Solvents for Synthesis and Catalysis. *Chem. Rev.* **1999**, *99*, 2071−2083.
(78) Wasserscheid, P.; Keim, W. Ionic Liquids - New "solutions" for Transition Metal Catalysis. *Angew. Chem., Int. Ed.* **2000**, *39*, 3772−3789.
(79) Parvulescu, V. I.; Hardacre, C. Catalysis in Ionic Liquids. *Chem. Rev.* **2007**, *107*, 2615−2665.
(80) Ye, C.; Liu, W.; Chen, Y.; Yu, L. Room-temperature Ionic Liquids: A Novel Versatile Lubricant. *Chem. Commun.* **2001**, 2244−2245.
(81) Liu, W.; Ye, C.; Gong, Q.; Wang, H.; Wang, P. Tribological Performance of Room-temperature Ionic Liquids as Lubricant. *Tribol. Lett.* **2002**, *13*, 81−85.
(82) Nainaparampil, J. J.; Eapen, K. C.; Sanders, J. H.; Voevodin, A. A. Ionic-liquid Lubrication of Sliding Mems Contacts: Comparison of Afm Liquid Cell and Device-level Tests. *J. Microelectromech. Syst.* **2007**, *16*, 836−843.
(83) Zhang, L.; Feng, D.; Xu, B. Tribological Characteristics of Alkylimidazolium Diethyl Phosphates Ionic Liquids as Lubricants for Steel-Steel Contact. *Tribol. Lett.* **2009**, *34*, 95−101.
(84) Palacio, M.; Bhushan, B. A Review of Ionic Liquids for Green Molecular Lubrication in Nanotechnology. *Tribol. Lett.* **2010**, *40*, 247−268.
(85) Antonietti, M.; Kuang, D.; Smarsly, B.; Zhou, Y. Ionic Liquids for The Convenient Synthesis of Functional Nanoparticles and Other Inorganic Nanostructures. *Angew. Chem., Int. Ed.* **2004**, *43*, 4988−4992.
(86) Pensado, A. S.; Padua, A. A. H. Solvation and Stabilization of Metallic Nanoparticles in Ionic Liquids. *Angew. Chem., Int. Ed.* **2011**, *50*, 8683−8687.
(87) Wang, B.; Wang, X.; Lou, W.; Hao, J. Ionic Liquid-based Stable Nanofluids Containing Gold Nanoparticles. *J. Colloid Interface Sci.* **2011**, *362*, 5−14.
(88) Ueno, K.; Watanabe, M. From Colloidal Stability in Ionic Liquids to Advanced Soft Materials Using Unique Media. *Langmuir* **2011**, *27*, 9105−9115.